HHS Public Access

Author manuscript

J Orthop Res. Author manuscript; available in PMC 2019 May 01.

Published in final edited form as:

J Orthop Res. 2018 May ; 36(5): 1356–1369. doi:10.1002/jor.23834.

RNA sequencing identifies gene regulatory networks controlling extracellular matrix synthesis in intervertebral disk tissues†

Scott M. Riester[1,2], **Yang Lin**[1,3], **Wei Wang**[1,4], **Lin Cong**[1,5], **Abdel-Moneim Mohamed Ali**[1], **Sun H. Peck**[6,7], **Lachlan J. Smith**[6,7], **Bradford L. Currier**[1], **Michelle Clark**[8], **Paul Huddleston**[1], **William Krauss**[8], **Michael J. Yaszemski**[1], **Mark E. Morrey**[1], **Matthew P. Abdel**[1], **Mohamad Bydon**[8], **Wenchun Qu**[9,10,11], **A. Noelle Larson**[1], **Andre J. van Wijnen**[1,*], and **Ahmad Nassr**[1,*]

[1]Department of Orthopedic Surgery, Mayo Clinic, Rochester, MN, USA

[2]Department of Occupational and Environmental Medicine, HealthPartners, MN, USA

[3]Department of Orthopedic Surgery, Tongji Hospital, Tongji Medical College, Huazhong University of Science and Technology, Wuhan, P.R. China

[4]Department of Orthopedic Surgery, Puai Hospital, Tongji Medical College, Huazhong University of Science and Technology, Wuhan, P.R. China

[5]Department of Orthopedic Surgery, The First Hospital of China Medical University, No.155, Nanjing Bei Street, Shenyang, 110001, P. R. China

[6]Department of Neurosurgery, Perelman School of Medicine, University of Pennsylvania, PA, USA

---

†This article has been accepted for publication and undergone full peer review but has not been through the copyediting, typesetting, pagination and proofreading process, which may lead to differences between this version and the Version of Record.

Corresponding Authors: Ahmad Nassr, M.D. & Andre J. van Wijnen, Ph.D., Mayo Clinic, 200 First Street SW, Rochester, MN 55905, Phone: 507- 538-0514, nassr.ahmad@mayo.edu; vanwijnen.andre@mayo.edu.

Additional Supporting Information may be found in the online version of this article.

Author Contributions:

Scott M. Riester - Carried out experiments, interpreted data, and helped draft and prepare final manuscript.
Yang Lin - Carried out experiments, and approved final manuscript.
Wei Wang - Carried out experiments, and approved final manuscript.
Sun H. Peck - assisted with technical design of study
Lachlan Smith - assisted with technical design of study, shared unpublished data and provided conceptual advice
Lin Cong - Carried out experiments, and approved final manuscript.
Abdel-Moneim Mohamed Ali - Interpreted data, and approved final manuscript.
Bradford Currier - Provided surgical specimens, and approved final manuscript.
Michelle Clark - Provided surgical specimens, and approved final manuscript.
Paul Huddleston - Provided surgical specimens, and approved final manuscript.
William Krauss - Provided surgical specimens, and approved final manuscript.
Michael J. Yaszemski - Provided surgical specimens, provided conceptual input and approved final manuscript.
Mark E. Morrey - Provided conceptual input, helped revise and approve final manuscript.
Matthew P. Abdel - Designed the study, provided conceptual input, helped revise and approve final manuscript.
Mohamad Bydon - Provided conceptual input, helped revise and approve final manuscript.
Wenchun Qu - Provided conceptual input, helped revise and approve final manuscript.
A. Noelle Larson - Assisted with design of the study, helped obtain funding, wrote introduction, helped revise and approve final manuscript.
Andre J. van Wijnen - Assisted with design of the study, provided funding for this project, helped revise and approve final manuscript.
Ahmad Nassr - Designed the study, provided funding for this project, provided surgical specimens for the study, helped draft revise and approve final manuscript.

The remaining authors have no conflicts relevant to this publication.

[7]Department of Orthopaedic Surgery, Perelman School of Medicine, University of Pennsylvania, PA, USA

[8]Department of Neurosurgery, Mayo Clinic, Rochester, MN, USA

[9]Department of Physical Medicine and Rehabilitation, Mayo Clinic, Rochester, MN, USA

[10]Department of Anesthesiology Division of Pain Medicine, Mayo Clinic, Rochester, MN, USA

[11]Spine Center, Mayo Clinic, Rochester, MN, USA

Abstract

Degenerative disk disease of the spine is a major cause of back pain and disability. Optimization of regenerative medical therapies for degenerative disk disease requires a deep mechanistic understanding of the factors controlling the structural integrity of spinal tissues. In this investigation, we sought to identify candidate regulatory genes controlling extracellular matrix synthesis in spinal tissues. To achieve this goal we performed high throughput next generation RNA sequencing on 39 annulus fibrosus and 21 nucleus pulposus human tissue samples. Specimens were collected from patients undergoing surgical discectomy for the treatment of degenerative disk disease. Our studies identified associations between extracellular matrix genes, growth factors, and other important regulatory molecules. The fibrous matrix characteristic of annulus fibrosus was associated with expression of the growth factors platelet derived growth factor beta (PDGFB), vascular endothelial growth factor C (VEGFC), and fibroblast growth factor 9 (FGF9). Additionally we observed high expression of multiple signaling proteins involved in the NOTCH and WNT signaling cascades. Nucleus pulposus extracellular matrix related genes were associated with the expression of numerous diffusible growth factors largely associated with the transforming growth signaling cascade, including transforming factor alpha (TGFA), inhibin alpha (INHA), inhibin beta A (INHBA), bone morphogenetic proteins (BMP2, BMP6), and others.

Keywords

RNA sequencing; nucleus pulposus; annulus fibrosus; intervertebral disk; extracellular matrix

Introduction

Back pain is among the leading global causes of disability[1, 2], with degenerative disk disease and osteoarthritis being important causes of disease. Disk degeneration is caused by a dysregulation of extracellular matrix homeostasis, characterized by dehydration of the central nucleus, reduced proteoglycan content, decreased cellularity, diminished endplate density, and disruption of the annulus[3–5]. Environmental exposures, as well as genetic and epigenetic factors have been associated with disk degeneration and altered extracellular matrix synthesis in disk tissues[6,7]. Novel molecular approaches that can target molecular factors regulating extracellular matrix synthesis in disk tissue have the potential to be used as therapeutic agents to slow or reverse disk degeneration in patients.

The molecular phenotype of intervertebral spinal disk tissue, including the annulus fibrosus (AF) and nucleus pulposus (NP), has been studied extensively in non-human animal models

for degenerative disk disease[8–14]. Studies evaluating transcriptome data using microarrays have provided us with an initial understanding of the molecular mechanisms underlying disk biology and have played a major role in helping to identify important biologic markers specific for AF and NP disk tissues[15–19]. However knowledge regarding the regulatory role of molecular factors and how they contribute to tissue homeostasis still requires further study.

In this investigation we seek to identify molecular regulatory factors whose transcriptional profiles correlate with the expression of extracellular matrix proteins important for the structural phenotype of human AF and NP tissues. To achieve this objective we evaluated transcriptome profiles of a cohort of human cervical disk tissue samples utilizing high throughput next generation RNA sequencing. We obtained complete gene expression profiles for 60 surgically harvested cervical disk specimens (AF and NP), and evaluated the main molecular landscapes of these two principal disc tissues. The large cohort of samples analyzed in this study allowed us to successfully perform weighted gene correlation analysis to identify gene regulatory clusters in disk tissues and assess gene relationships.

The molecular regulators that show relationships with extracellular matrix gene expression represent promising candidates for future study and therapeutic validation. The findings in this investigation also serve to support regenerative medicine therapies currently under development for the treatment of intervertebral disk disease, including stem cell therapies and tissue engineering strategies to regrow disk tissue for surgical transplantation and disk replacement procedures[20,21]. Both of these strategies require a comprehensive definition of the molecular phenotype of the human intervertebral disk to evaluate the efficacy of strategies to differentiate stem cells or engineer tissue disk tissue in vivo. The transcriptional signatures and gene relationships identified in this study have broad applicability in both the stem cell and tissue engineering fields.

Methods

Surgical tissue collection

A total of 60 tissue specimens were collected for research use from 48 adult patients undergoing cervical discectomy. Patients ranged in age from 32 to 77 years of age and included a balanced distribution of male and female patients (Supplemental Table 1). Patients in this study underwent surgery for the treatment of symptomtic degenerative disk disease presenting with or without myelopathy. Subjects were enrolled in the study in the period between January 2011 and April 2015. Cases in which discectomy was performed in the setting of acute trauma or infection were excluded from this study. At the time of tissue collection, the AF and NP were carefully dissected from one another in the operating room by the staff surgeon. In cases where disc degeneration was severe, NP tissue could not always be readily identified and distinguished from the AF tissue and therefore could not be collected for some patients. At the time of surgical harvest, tissues were snap frozen in liquid nitrogen and stored at −80°C until ready for RNA extraction. All samples were frozen within 40 minutes of removal from the patient. Grade of disk degeneration was evaluated on preoperative lateral radiographs and was characterized using the classification described by Lane et al.[22,23]. Clinical data available for each disk sample is provided in Supplemental

Table 1. The specimens used in this investigation were collected under institutional review board approved protocols (IRB#10–005713). Written informed consent was obtained for all biospecimens that were analyzed.

RNA extraction from intervertebral disk tissue

Frozen tissue biopsies were ground into a powder using a mortar and pestle and homogenized in Qiazol reagent (Qiagen, Hilden, Germany) and homogenized. Total RNA was extracted from research biopsies based on previous methods[24, 25] using the miRNeasy minikit (Qiagen, Hilden, Germany) and quantified using the NanoDrop 2000 spectrophotometer (Thermo Fischer Scientific, Wilmington, Delaware). For samples selected for next generation sequencing, RNA integrity was assessed using the Agilent Bioanalyzer DNA 1000 chip (Invitrogen, Carlsbad, CA).

Next generation mRNA sequencing, statistics and bioinformatics

RNA sequencing and bioinformatics analyses were performed as previously described[26–29]. In brief, library preparation was performed using the TruSeq RNA library preparation kit (Illumina, San Diego, CA). Polyadenylated mRNAs were selected using oligo dT magnetic beads. TruSeq Kits (12-Set A and 12-Set B) were used for indexing to permit multiplex sample loading on the flow cells. Paired-end sequencing reads were generated on the Illumina HiSeq 2000 sequencer. Quality control for concentration and library size distribution was performed using an Agilent Bioanalyzer DNA 1000 chip and Qubit fluorometry (Invitrogen, Carlsbad, CA). Sequence alignment of reads and determination of normalized gene counts were performed using the MAP-RSeq (v.1.2.1) workflow[30], utilizing TopHat 2.0.6[31, 32], and HTSeq[33].

RNA sequencing data were analyzed to assess relevant genes that differ between AF and NP specimens. Genes with a minimal expression value (RPKM > 0.01) were included in subsequent computational analysis. Fold-change differences in gene expression were evaluated using the Mann-Whitney U test with a 1% false discovery rate (FDR), and statistical significance was set at $p < 0.05$. Unsupervised hierarchical clustering was performed using the Pearson correlation method. Weighted gene correlation analysis was performed using the R package WGCNA (Weighted Gene Correlation Analysis)[34]. Genes with an average RPKM expression > 0.01 across all specimens were included in the computational analysis. Functional gene annotation classification of WGCNA clusters was performed using DAVID Bioinformatics Resources 6.7 database (DAVID 6.7)[35].

Results

RNA sequencing was performed using 60 unique cervical spine disk tissue samples (39 AF and 21 NP specimens). High quality sequencing reads were obtained for 57 of the 60 samples. The 3 samples with abnormally low read counts were excluded from further analysis. To detect sample outliers, an unbiased assessment of transcriptome data using unsupervised hierarchical clustering was performed. This analysis revealed 10 disk samples that clustered independently from the majority of the disk specimens (Supplemental Figure 1). A comparison of these samples with specimens in the primary cluster show that outlier

samples express higher levels of blood related genes including genes linked to the erythroid, lymphoid, and myeloid lineages. A selective evaluation of the blood specific hemoglobin genes, hemoglobin subunit beta (HBB), hemoglobin subunit alpha 1 (HBA1), and hemoglobin subunit alpha 2 (HBA2), confirmed that these 10 samples express the highest levels of blood related genes (Supplemental Table 2). To ensure the comparability of samples in our study these outliers were removed from subsequent analysis. Repeated unsupervised hierarchical clustering after removal of outliers showed an expected trend toward independent clustering of AF and nucleus puplosus tissue samples (Figure 1a). Genes that are not strictly linked to a tissue phenotype such as hematopoietic and inflammation related genes, as well as tissue heterogeneity, played a role in defining the clustering dendrogram. This observation explains why the clustering dendrogram showed a trending, but not completely independent clustering of the AF and NP specimens, despite the distinct biological phenotypes of AF and NP tissues.

An examination of the most highly expressed genes (expression > 100 RPKM) commonly expressed in AF and NP expectedly showed common enrichment of genes associated with housekeeping functions (i.e. translation, protein ubiquitination) (Figure 1b). The AF and NP samples share many ECM related genes in common among their highest expressed genes, however the abundance of each gene and their ratios are quite different between AF and NP samples. Of the genes that are commonly enriched in AF and NP that are not associated with house-keeping functions, the AF samples showed higher expression of mRNAs encoding ECM proteins associated with a fibrous matrix including type I collagen (COL1A2), and type VI collagen (COL6A1, COL6A2, COL6A3) (Table 1). In contrast, the NP samples showed increased mRNA levels of genes encoding extracellular matrix proteins associated with a proteoglycan rich chondrogenic matrix, including cartilage oligomeric protein (COMP), lumican (LUM), type II collagen (COL2A1), cartilage intermediate layer protein (CILP), biglycan (BGN), aggrecan (ACAN), type III collagen (COL3A1), chondroadherin (CHAD), and others (Table 2)

To determine genes that are differentially expressed between AF and NP tissues irrespective of their overall abundance, a fold-change comparison of gene expression data in AF and NP was performed. We observed statistically significant enrichment of 1399 genes in AF tissue and 373 genes with enrichment in NP tissue (Supplemental Table 3). Analysis revealed differential gene expression consistent with the biological properties and function of each tissue type. The AF showed enrichment in genes linked to adhesion and regulation of cell contact, consistent with its fibrous structural properties (Figure 1c). In contrast, the NP samples showed enrichment in mRNAs associated with proteoglycan extracellular matrix synthesis, including genes associated with the endoplasmic reticulum and Golgi apparatus (Figure 1d). These findings are consistent with the functional role of the NP, which acts as a hydrostatic cushion to reduce contact pressure between the bony vertebral bodies of the spine. We also observed preferential expression of the notochord specific transcription factor brachyury (T) in NP tissues at low, but detectable levels in about half of the samples. This indicates that residual notochord cell populations, detectable when highly sensitive molecular techniques are applied, may be present in degenerative adult disc tissue.

The AF and NP specimens both showed statistically significant enrichment in known, as well as novel, extracellular matrix proteins and signaling molecules. The AF specimens showed expression of phenotypically important genes such as type IV collagen (COL4A1), multiple laminins important for cell adhesion (LAMA3, LAMA4, LAMA5), and genes linked to NOTCH signaling (DLL1, JAG1, JAG2, NOTCH3, NOTCH4). In NP specimens we observed expression of genes promoting a proteoglycan rich ECM including aggrecan (ACAN), type XI collagen (COL11 A1), glypican 6 (GPC6), lumican (LUM), among others in NP specimens (Table 3).

Given the heterogeneous nature of spinal tissues, statistical methods used to assess simple fold-change analyses may not always be able to identify all important biological gene relationships. To overcome this challenge and identify novel gene regulatory networks with a functional role in regulating extracellular matrix production, we performed weighted gene correlation network analysis for spine tissues using the R package WGCNA[34]. Gene correlation analysis identified 46 regulatory gene clusters present in our intervertebral disk samples (Figure 2). We observed gene regulatory clusters associated with housekeeping functions (i.e. translation, transcription, mitochondrion, nuclear homeostasis), cellular infiltration including blood and inflammatory cells. We also observed gene regulatory clusters associated with non-disk tissue including processes related to muscle, bone, and adipogenesis, which likely represent small quantities of tissue mixed in with disk tissue at the time of surgical harvesting.

To identify novel extracellular matrix proteins and regulatory molecules that control tissue specific phenotypes, we examined clusters containing genes associated extracellular matrix synthesis. The related clusters “paleturquoise”, “darkorange2”, and “darkslateblue” each show enrichment in extracellular matrix proteins and adhesive proteins associated with a fibrous matrix, which is typically characteristic of AF tissue. These clusters contain genes that promote a strong fibrous matrix, including collagens, fibulins, integrins, lamamins, elastin, and others (Table 4). These gene clusters were notably associated with a three diffusible growth factors, fibroblast growth factor 9 (FGF9), platelet-derived growth factor beta polypeptide (PDGFB), and vascular endothelial growth factor C (VEGFC). These findings suggest that these growth factors may play a regulatory roles in maintenance of the AF phenotype and warrant further investigation. Additionally, these clusters also exhibited strong enrichment in genes linked to cell-cell signaling interactions, including the Wnt signaling and NOTCH signaling pathways. Both of these pathways are known to be involved in mediating cell-cell interactions and cellular adhesion in various tissues outside of intervertebral disk[36, 37]. Given the paucity of diffusible growth factors and the fact that AF cells are in close contact with one another, these data suggest that AF ECM production may be regulated or strongly influenced by direct cell-cell signaling mechanisms, possibly mediated through the Wnt and NOTCH signaling pathways.

The clusters “black”, “grey60”, and “lightyellow” show enrichment in genes associated with a proteoglycan rich extracellular matrix. Genes included in these clusters include the known NP markers type II collagen (COL2A1), type IX collagens (COL9A2, COL9A3), type XI collagen (COL11A2), aggrecan (ACAN), as well as other genes associated with a proteoglycan rich ECM that have not previously been associated with NP phenotype (Table

5). In contrast to the gene clusters previously discussed that were associated with synthesis of a fibrous matrix, these gene clusters express a diverse array of diffusible growth factors, with many being associated with the TGFβ signaling cascade. Associated growth factors include transforming growth factor alpha (TGFA), inhibin beta A (INHBA), inhibin alpha (INHA), growth differentiation factors (GDF5, GDF6), and bone morphogenetic proteins (BMP2, BMP6) and others (Table 5). The reliance on diffusible growth factors to mediate ECM homeostasis in a proteoglycan rich matrix such as that observed in the NP is logical since cells are usually separated by a thick matrix and have limited direct cell to cell contact. A comprehensive list of the genes associated with each regulatory cluster showing enrichment in either AF (fibrous) or NP (proteoglycan) markers are shown in Supplemental Table 4.

Discussion

The molecular phenotype of intervertebral spinal disk tissue, including the AF and NP, has been studied extensively over the past several years, primarily in animal models. The disk periphery is comprised of the fibrous annulus, derived from the scleroderm, while NP is derived from the notochord. However, notochordal cells in humans decrease in abundance with age, and are largely absent after adolescence[38, 39], although visible notochord tissue is present at maturity in other species. NP cells make predominantly type II collagen, whereas AF cells make both type I and type II collagen[40]. The findings in our investigation utilizing high throughput RNA sequencing approaches are consistent with these findings in previous investigations, and also identify associations with other novel extracellular matrix proteins and associated regulatory factors.

Our initial clustering analysis performed using AF and NP specimens (Figure 1) demonstrates that blood content is an important consideration in the evaluation of surgically collected spinal disk tissues. Disk tissues have a very low density of cells, and the few cells that are present are usually encased in a thick extracellular matrix that makes RNA extraction technically challenging. Even the presence of small quantities of blood, from which RNA is much more easily extracted, can profoundly impact RNA content and resulting transcriptome data analyses if not carefully considered.

Our analysis reveals increased expression of known AF and NP markers within corresponding tissue types including enrichment of type I collagen in AF and a proteoglycan associated extracellular matrix enriched in genes such as ACAN, COMP, LUM, and others in the NP. We note that there is some overlap in mRNA expression between annulus and nucleus specimens. This overlap may reflect similarities in the developmental origin of these tissues or could be due to technical issues, for example, because there is some intermixing of annulus and nucleus cells during tissue harvest (e.g., in degenerative disk tissues with altered structural morphology).

These studies also implicate the WNT and NOTCH signaling pathway as a potentially important regulators of cell adhesion and matrix synthesis in AF tissue. These pathways are mediated by direct cell to cell interactions and have been shown to impact cellular adhesion and tissue integrity in various tissue types[41]. Golgi and ER related genes enriched in NP

tissue may contribute to the production of the proteogylcan rich matrix associated with the NP environment. Therapeutic strategies that can increase protein output and upregulate the expression of NP specific genes have the potential to help disk tissue retain fluid and appropriate hydrostatic pressure, thus preventing disk space degeneration and associated disk space narrowing and osteoarthritis.

Recent studies have identified several novel AF and NP markers, our study shows support for many of these markers[42]. In our analyses, the proposed NP markers desmocollin 2 (DSC2)[18], lubricin (PRG4)[43], and paired box 1 (PAX1)[20], showed co-regulation with networks enriched in NP related genes supporting their classification as NP markers. The novel AF markers brain abundant membrane attached signal protein 1 (BASP1), sclerostin domain containing 1 (SOSTDC1)[18], glypican 3 (GPC3), and pleiotrophin (PTN)[44] also showed co-regulation with AF related ECM gene networks. Our study did not show a clear link to either AF or NP phenotypes for several published markers including CD24 antigen (CD24), keratin 8 (KRT8), keratin 18 (KRT18), keratin 19 (KRT19), cadherin 2 (CDH2)[17], carbonic anhydrase 12 (CA12)[45], and hypoxia inducible factor 1 alpha subunit (HIF1A)[13, 14, 46], all of which showed co-regulation with gene networks unrelated to disk phenotype. Protein levels do not always correlate with mRNA expression, which could explain some of the differences between our study and previous investigations. Discrepancies could also be related to interspecies differences, as many of these published studies were carried out using non-human tissues. In addition, our study focused on evaluation of degenerative disc tissue, and it is possible that many of these markers may be present during early disk development and are gradually lost over time with aging and degeneration.

It is important to note that the gene relationships defined by network analyses in this study may exclude important functional/regulatory genes when a gene has a stronger relationship to another network. This was observed for the known AF related gene type I collagen (COL1 A1, COL1A2), which showed stronger co-regulation with bone related genes (gene cluster “royalblue”) rather than AF related genes. Despite this limitation, we were still able to identify large gene regulatory networks associated with ECM production in AF and NP tissues. Our analysis also does not take in account the numerous regulatory mechanisms that act in coordination with transcriptional mechanisms including protein phosphorylation and acetylation, histone modifications, microRNAs, and others. Future studies that integrate intervertebral disk transcriptomic profiles with various types of molecular data including microRNA profiles, and mass spectroscopy data may further help to elucidate novel molecular pathways involved intervertebral disk homeostasis.

This investigation provides a comprehensive overview of mRNA expression in annulus fibrosus and nucleus pulposus intervertebral disk tissue, including extracellular matrix components. By applying computational analyses to our large dataset of human clinical specimens, we have been able to identify candidate gene regulatory networks that act in AF and NP tissues to regulate extracellular matrix synthesis, an important determinant of intervertebral disk integrity. The transcriptome data generated in this study also serves as an important reference data set and has the potential to help solve many biological questions related to disk tissues. For example, our data can be used to evaluate the efficacy of tissue

engineering strategies for intervertebral disk development. The data can also be applied to optimize stem cell differentiation strategies for therapeutic disk regeneration, as a variety of stem cell therapies are just beginning to be investigated in new clinical trials. Information generated in this study can also potentially be applied to identify novel therapeutic targets to enhance extracellular matrix synthesis and restore the normal mechanical properties of intervertebral disk tissue.

Supplementary Material

Refer to Web version on PubMed Central for supplementary material.

Acknowledgments

This publication was made possible by grants from the Cervical Spine Research Society (21st Century grant; to AN) and the generous philanthropic support of William and Karen Eby. Additional support was provided by the National Institutes of Health, including the National Institute of Arthritis and Musculoskeletal and Skin Diseases (NIAMS, R03 AR066342, to ANL; R01 AR049069, to AvW) and the National Center for Advancing Translational Sciences (NCATS), a component of the National Institutes of Health (CTSA Grant Number UL1 TR000135, to ANL). Funding was also provided by the Mayo Graduate School (to SMR) through CTSA Grant Number UL1 TR000135 from the National Center for Advancing Translational Sciences. Additional support was also provided by the Doctor Research Startup Fund' of Liaoning Province (Grant#201601114; to LC). We also thank the members of our research groups, including Emily Camilleri and Amel Dudakovic for stimulating discussions, as well as the Mayo Clinic Bioinformatics Core, including Jared Evans and Asha Nair for their assistance with high-throughput RNA sequencing and bioinformatics support. Dr. Bradford Currier owns stock in Spinology and Tenex, and is on the Board of Directors for the Lumbar Spine Research Society.

References

1. Global Burden of Disease Study C. Global, regional, and national incidence, prevalence, and years lived with disability for 301 acute and chronic diseases and injuries in 188 countries, 1990–2013: a systematic analysis for the Global Burden of Disease Study 2013. Lancet. 2015; 386(9995):743–800. PubMed PMID: 26063472; PMCID: PMC4561509. DOI: 10.1016/S0140-6736(15)60692-4 [PubMed: 26063472]
2. Driscoll T, Jacklyn G, Orchard J, et al. The global burden of occupationally related low back pain: estimates from the Global Burden of Disease 2010 study. Ann Rheum Dis. 2014; 73(6):975–81. PubMed PMID: 24665117. DOI: 10.1136/annrheumdis-2013-204631 [PubMed: 24665117]
3. Videman T, Sarna S, Battie MC, et al. The long-term effects of physical loading and exercise lifestyles on back-related symptoms, disability, and spinal pathology among men. Spine. 1995; 20(6):699–709. PubMed PMID: 7604346. [PubMed: 7604346]
4. Roughley PJ, Alini M, Antoniou J. The role of proteoglycans in aging, degeneration and repair of the intervertebral disc. Biochem Soc Trans. 2002; 30(Pt 6):869–74. doi: 10.1042/. PubMed PMID: 12440935. [PubMed: 12440935]
5. Rodriguez AG, Rodriguez-Soto AE, Burghardt AJ, et al. Morphology of the human vertebral endplate. Journal of orthopaedic research : official publication of the Orthopaedic Research Society. 2012; 30(2):280–7. PubMed PMID: 21812023; PMCID: PMC3209496. DOI: 10.1002/jor.21513 [PubMed: 21812023]
6. Roberts S, Evans H, Trivedi J, et al. Histology and pathology of the human intervertebral disc. The Journal of bone and joint surgery American volume. 2006; 88(Suppl 2):10–4. PubMed PMID: 16595436. DOI: 10.2106/JBJS.F.00019
7. Battie MC, Videman T, Gill K, et al. 1991 Volvo Award in clinical sciences. Smoking and lumbar intervertebral disc degeneration: an MRI study of identical twins. Spine. 1991; 16(9):1015–21. PubMed PMID: 1948392. [PubMed: 1948392]
8. Gilson A, Dreger M, Urban JP. Differential expression level of cytokeratin 8 in cells of the bovine nucleus pulposus complicates the search for specific intervertebral disc cell markers. Arthritis Res

Ther. 2010; 12(1):R24. PubMed PMID: 20152014; PubMed Central PMCID: PMC2875658. doi: 10.1186/ar2931 [PubMed: 20152014]

9. Yang F, Leung VY, Luk KD, et al. Injury-induced sequential transformation of notochordal nucleus pulposus to chondrogenic and fibrocartilaginous phenotype in the mouse. J Pathol. 2009 May; 218(1):113–21. PubMed PMID: 19288580. DOI: 10.1002/path.2519 [PubMed: 19288580]
10. Kim KW, Lim TH, Kim JG, et al. The origin of chondrocytes in the nucleus pulposus and histologic findings associated with the transition of a notochordal nucleus pulposus to a fibrocartilaginous nucleus pulposus in intact rabbit intervertebral discs. Spine (Phila Pa 1976). 2003 May 15; 28(10):982–90. PubMed PMID: 12768135. [PubMed: 12768135]
11. Agrawal A, Gajghate S, Smith H, et al. Cited2 modulates hypoxia-inducible factor-dependent expression of vascular endothelial growth factor in nucleus pulposus cells of the rat intervertebral disc. Arthritis Rheum. 2008 Dec; 58(12):3798–808. PubMed PMID: 19035510. DOI: 10.1002/art.24073 [PubMed: 19035510]
12. Agrawal A, Guttapalli A, Narayan S, et al. Normoxic stabilization of HIF-1alpha drives glycolytic metabolism and regulates aggrecan gene expression in nucleus pulposus cells of the rat intervertebral disk. Am J Physiol Cell Physiol. 2007 Aug; 293(2):C621–31. PubMed PMID: 17442734. [PubMed: 17442734]
13. Gogate SS, Nasser R, Shapiro IM, et al. Hypoxic regulation of β-1,3-glucuronyltransferase 1 expression in nucleus pulposus cells of the rat intervertebral disc: role of hypoxia-inducible factor proteins. Arthritis Rheum. 2011 Jul; 63(7):1950–60. PubMed PMID: 21400481; PubMed Central PMCID: PMC3125401. DOI: 10.1002/art.30342 [PubMed: 21400481]
14. Smolders LA, Meij BP, Onis D, et al. Gene expression profiling of early intervertebral disc degeneration reveals a down-regulation of canonical Wnt signaling and caveolin-1 expression: implications for development of regenerative strategies. Arthritis Res Ther. 2013 Jan 29.15(1):R23. PubMed PMID: 23360510; PubMed Central PMCID: PMC3672710. doi: 10.1186/ar4157 [PubMed: 23360510]
15. Minogue BM, Richardson SM, Zeef LA, et al. Transcriptional profiling of bovine intervertebral disc cells: implications for identification of normal and degenerate human intervertebral disc cell phenotypes. Arthritis Res Ther. 2010; 12(1):R22. PubMed PMID: 20149220; PubMed Central PMCID: PMC2875656. doi: 10.1186/ar2929 [PubMed: 20149220]
16. Sakai D, Nakai T, Mochida J, et al. Differential phenotype of intervertebral disc cells: microarray and immunohistochemical analysis of canine nucleus pulposus and anulus fibrosus. Spine (Phila Pa 1976). 2009 Jun 15; 34(14):1448–56. PubMed PMID: 19525835. DOI: 10.1097/BRS.0b013e3181a55705 [PubMed: 19525835]
17. Chen K, Wu D, Zhu X, et al. Gene expression profile analysis of human intervertebral disc degeneration. Genet Mol Biol. 2013 Sep; 36(3):448–54. PubMed PMID: 24130454; PubMed Central PMCID: PMC3795174. DOI: 10.1590/S1415-47572013000300021 [PubMed: 24130454]
18. Minogue BM, Richardson SM, Zeef LA, et al. Characterization of the human nucleus pulposus cell phenotype and evaluation of novel marker gene expression to define adult stem cell differentiation. Arthritis Rheum. 2010 Dec; 62(12):3695–705. PubMed PMID: 20722018. DOI: 10.1002/art.27710 [PubMed: 20722018]
19. Tang Y, Wang S, Liu Y, et al. Microarray analysis of genes and gene functions in disc degeneration. Exp Ther Med. 2014 Feb; 7(2):343–348. PubMed PMID: 24396401; PubMed Central PMCID: PMC3881058. [PubMed: 24396401]
20. Gilbert HT, Hoyland JA, Richardson SM. Stem cell regeneration of degenerated intervertebral discs: current status (update). Curr Pain Headache Rep. 2013 Dec.17(12):377. Review. PubMed PMID: 24234817. doi: 10.1007/s11916-013-0377-0 [PubMed: 24234817]
21. Tong W, Lu Z, Qin L, Mauck RL, et al. Cell therapy for the degenerating intervertebral disc. Transl Res. 2016 Nov 28. pii: S1931-5244(16)30403-0. [Epub ahead of print] Review. PubMed PMID: 27986604. doi: 10.1016/j.trsl.2016.11.008
22. Kettler A, Wilke HJ. Review of existing grading systems for cervical or lumbar disc and facet joint degeneration. Eur Spine J. 2006 Jun; 15(6):705–18. Epub 2005 Sep 20. Review. Erratum in: Eur Spine J. 2006 Jun;15(6):719. PubMed PMID:16172902; PubMed Central PMCID: PMC3489462. [PubMed: 16172902]

23. Lane NE, Nevitt MC, Genant HK, Hochberg MC. Reliability of new indices of radiographic osteoarthritis of the hand and hip and lumbar disc degeneration. J Rheumatol. 1993 Nov; 20(11): 1911–8. PubMed PMID: 8308778. [PubMed: 8308778]
24. Peck SH, O'Donnell PJ, Kang JL, et al. Delayed hypertrophic differentiation of epiphyseal chondrocytes contributes to failed secondary ossification in mucopolysaccharidosis VII dogs. Mol Genet Metab. 2015 Nov; 116(3):195–203. PubMed PMID: 26422116; PubMed Central PMCID:PMC4641049. DOI: 10.1016/j.ymgme.2015.09.008 [PubMed: 26422116]
25. Peck SH, Casal ML, Malhotra NR, et al. Pathogenesis and treatment of spine disease in the mucopolysaccharidoses. Mol Genet Metab. 2016 Aug; 118(4):232–43. Review. PubMed PMID: 27296532; PubMed Central PMCID: PMC4970936. DOI: 10.1016/j.ymgme.2016.06.002 [PubMed: 27296532]
26. Camilleri ET, Gustafson MP, Dudakovic A, et al. Identification and validation of multiple cell surface markers of clinical-grade adipose-derived mesenchymal stromal cells as novel release criteria for good manufacturing practice-compliant production. Stem Cell Res Ther. 2016 Aug 11.7(1):107. PubMed PMID: 27515308; PubMed Central PMCID: PMC4982273. doi: 10.1186/s13287-016-0370-8 [PubMed: 27515308]
27. Lin Y, Lewallen EA, Camilleri ET, et al. RNA-seq analysis of clinical-grade osteochondral allografts reveals activation of early response genes. J Orthop Res. 2016 Feb 22. [Epub ahead of print] PubMed PMID: 26909883; PubMed Central PMCID: PMC4993686. doi: 10.1002/jor.23209
28. Dudakovic A, Camilleri ET, Xu F, et al. Epigenetic Control of Skeletal Development by the Histone Methyltransferase Ezh2. J Biol Chem. 2015 Nov 13; 290(46):27604–17. Epub 2015 Sep 30. PubMed PMID:26424790; PubMed Central PMCID: PMC4646012. DOI: 10.1074/jbc.M115.672345 [PubMed: 26424790]
29. Eirin A, Riester SM, Zhu XY, et al. MicroRNA and mRNA cargo of extracellular vesicles from porcine adipose tissue-derived mesenchymal stem cells. Gene. 2014 Nov 1; 551(1):55–64. Epub 2014 Aug 23. PubMed PMID: 25158130; PubMed Central PMCID: PMC4174680. DOI: 10.1016/j.gene.2014.08.041 [PubMed: 25158130]
30. Kalari KR, Nair AA, Bhavsar JD, et al. MAP-RSeq: Mayo Analysis Pipeline for RNA sequencing. BMC Bioinformatics. 2014 Jun 27.15:224. PubMed PMID: 24972667; PubMed Central PMCID: PMC4228501. doi: 10.1186/1471-2105-15-224 [PubMed: 24972667]
31. Langmead B, Trapnell C, Pop M, et al. Ultrafast and memory-efficient alignment of short DNA sequences to the human genome. Genome Biol. 2009; 10(3):R25. PubMed PMID: 19261174; PubMed Central PMCID: PMC2690996. doi: 10.1186/gb-2009-10-3-r25 [PubMed: 19261174]
32. Kim D, Pertea G, Trapnell C, et al. TopHat2: accurate alignment of transcriptomes in the presence of insertions, deletions and gene fusions. Genome Biol. 2013 Apr 25.14(4):R36. PubMed PMID: 23618408; PubMed Central PMCID: PMC4053844. doi: 10.1186/gb-2013-14-4-r36 [PubMed: 23618408]
33. Anders S, Pyl PT, Huber W. HTSeq--a Python framework to work with high-throughput sequencing data. Bioinformatics. 2015 Jan 15; 31(2):166–9. PubMed PMID: 25260700; PubMed Central PMCID: PMC4287950. DOI: 10.1093/bioinformatics/btu638 [PubMed: 25260700]
34. Langfelder P, Horvath S. WGCNA: an R package for weighted correlation network analysis. BMC Bioinformatics. 2008 Dec 29.9:559. PubMed PMID: 19114008; PubMed Central PMCID: PMC2631488. doi: 10.1186/1471-2105-9-559 [PubMed: 19114008]
35. Huang da W, Sherman BT, Lempicki RA. Systematic and integrative analysis of large gene lists using DAVID bioinformatics resources. Nat Protoc. 2009; 4(1):44–57. PubMed PMID: 19131956. DOI: 10.1038/nprot.2008.211 [PubMed: 19131956]
36. Sanson B, White P, Vincent JP. Uncoupling cadherin-based adhesion from wingless signalling in Drosophila. Nature. 1996 Oct 17; 383(6601):627–30. PubMed PMID: 8857539. [PubMed: 8857539]
37. Gonzalez DM, Medici D. Signaling mechanisms of the epithelial-mesenchymal transition. Sci Signal. 2014 Sep 23.7(344):re8. Review. PubMed PMID: 25249658; PubMed Central PMCID: PMC4372086. doi: 10.1126/scisignal.2005189 [PubMed: 25249658]
38. Smith LJ, Nerurkar NL, Choi KS, et al. Degeneration and regeneration of the intervertebral disc: lessons from development. Dis Model Mech. 2011 Jan; 4(1):31–41. Review. PubMed PMID:

21123625; PubMed Central PMCID: PMC3008962. DOI: 10.1242/dmm.006403 [PubMed: 21123625]

39. Pazzaglia UE, Salisbury JR, Byers PD. Development and involution of the notochord in the human spine. J R Soc Med. 1989; 82(7):413–5. PubMed PMID: 2585428; PMCID: PMC1292207. [PubMed: 2585428]
40. Chelberg MK, Banks GM, Geiger DF, et al. Identification of heterogeneous cell populations in normal human intervertebral disc. Journal of anatomy. 1995; 186(Pt 1):43–53. PubMed PMID: 7544335; PMCID: PMC1167271. [PubMed: 7544335]
41. Sprinzak D, Lakhanpal A, Lebon L, et al. Cis-interactions between Notch and Delta generate mutually exclusive signalling states. Nature. 2010 May 6; 465(7294):86–90. Epub 2010 Apr 25. PubMed PMID: 20418862; PubMed Central PMCID: PMC2886601. DOI: 10.1038/nature08959 [PubMed: 20418862]
42. Risbud MV, Schoepflin ZR, Mwale F, et al. Defining the phenotype of young healthy nucleus pulposus cells:recommendations of the Spine Research Interest Group at the 2014 annual ORS meeting. J Orthop Res. 2015 Mar; 33(3):283–93. PubMed PMID: 25411088; PubMed Central PMCID: PMC4399824. DOI: 10.1002/jor.22789 [PubMed: 25411088]
43. Önnerfjord P, Khabut A, Reinholt FP, et al. Quantitative proteomic analysis of eight cartilaginous tissues reveals characteristic differences as well as similarities between subgroups. J Biol Chem. 2012 Jun 1; 287(23):18913–24. PubMed PMID: 22493511; PubMed Central PMCID: PMC3365926. DOI: 10.1074/jbc.M111.298968 [PubMed: 22493511]
44. Lee CR, Sakai D, Nakai T, et al. A phenotypic comparison of intervertebral disc and articular cartilage cells in the rat. Eur Spine J. 2007; 16:2174–2185. [PubMed: 17786487]. [PubMed: 17786487]
45. Power KA, Grad S, Rutges JP, et al. Identification of cell surface-specific markers to target human nucleus pulposus cells: expression of carbonic anhydrase XII varies with age and degeneration. Arthritis Rheum. 2011 Dec; 63(12):3876–86. PubMed PMID: 22127705. DOI: 10.1002/art.30607 [PubMed: 22127705]
46. Risbud MV, Guttapalli A, Stokes DG, et al. Nucleus pulposus cells express HIF-1 alpha under normoxic culture conditions: a metabolic adaptation to the intervertebral disc microenvironment. J Cell Biochem. 2006 May 1; 98(1):152–9. PubMed PMID: 16408279. [PubMed: 16408279]

Clinical Significance

This investigation provides important data on extracellular matrix gene regulatory networks in disk tissues. This information can be used to optimize pharmacologic, stem cell, and tissue engineering strategies for regeneration of the intervertebral disk and the treatment of back pain.

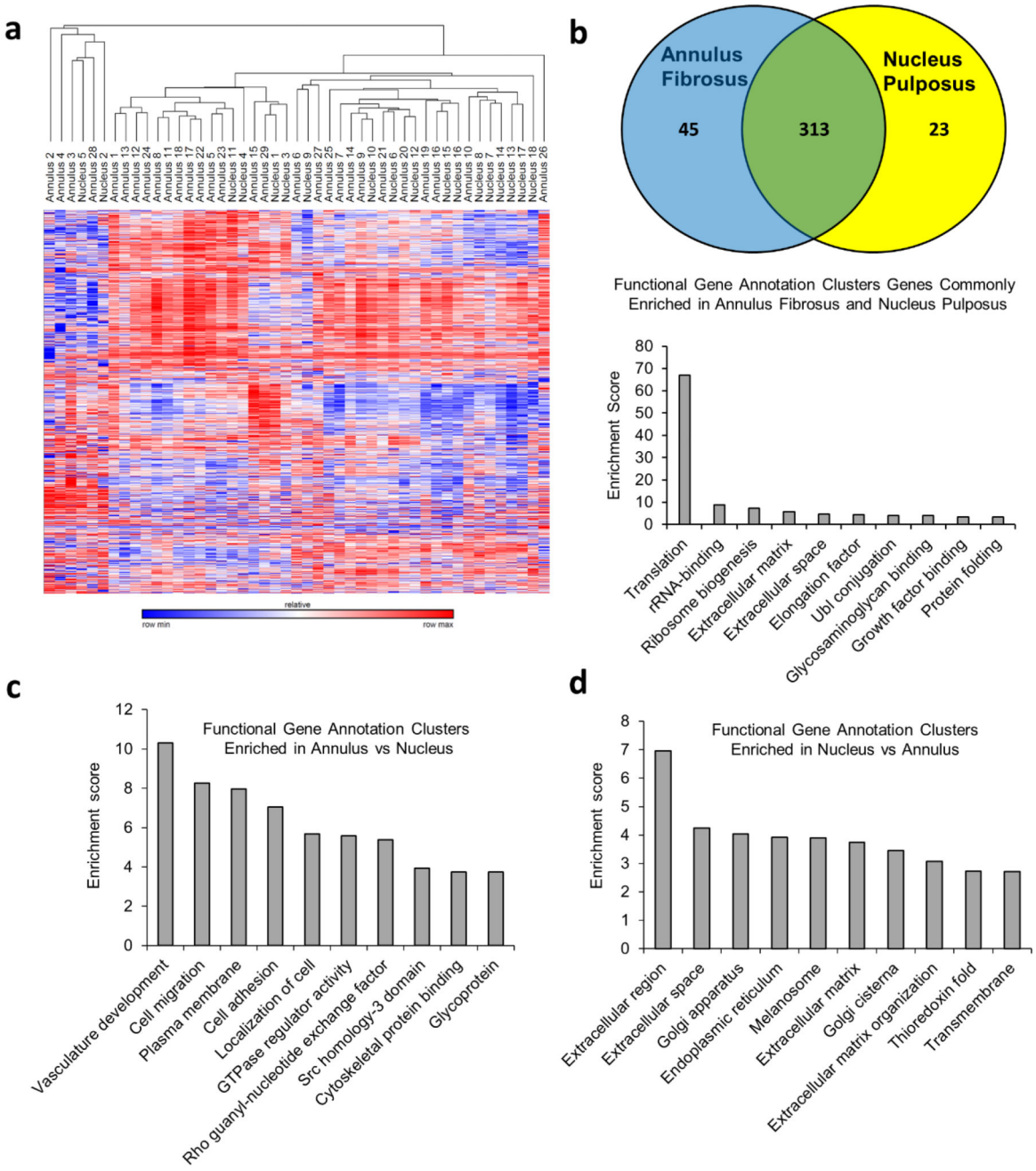

Figure 1.

(a) Unsupervised hierarchical clustering of RNA sequencing data after removal of sample outliers. In this clustering scheme there is a trend for AF and NP samples to preferentially cluster separately. These findings suggest that there are tissue specific differences contained within the transcriptome data, representing the known biological differences that exist between these two tissue types. Our unbiased approach also incorporates various factors that are not directly related to the disc phenotype such as tissue heterogeneity, blood content, and inflammation, which can drive some of the biological variation between specimens, thus precluding a perfect clustering dendogram in which AF and NP specimens cluster as

completely independent groups. (b) Genes expressed > 100 RPKM in surgically isolated AF and NP tissue with equal expression levels (Fold change <1.5 between AF and NP). This analysis shows that AF and NP both share common expression of a large number of housekeeping genes as well as a small number of extracellular matrix proteins and growth factor binding associated proteins. (c) Gene ontology analysis reveals enrichment in pathways that promote cellular adhesion including genes linked to notch signaling (vasculature development, GTPase regulator activity) in AF tissue. (d) The NP shows enrichment in genes linked to extracellular matrix protein synthesis, including in genes controlling the extracellular matrix protein synthesis machinery (golgi complex and endoplasmic reticulum).

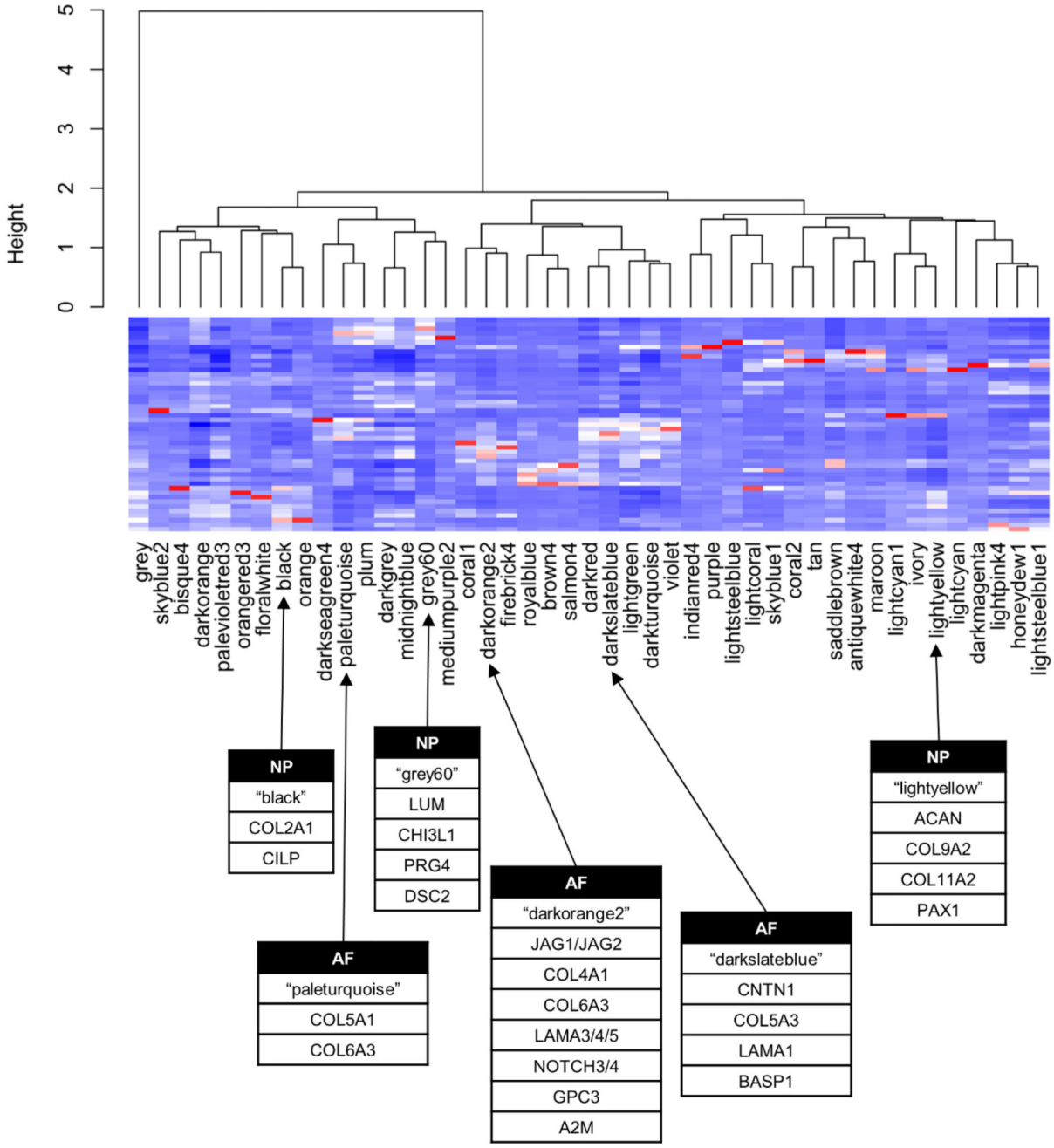

Figure 2.

Gene correlation networks predicted using weighted genes correlation analysis (WGCNA). Gene networks are associated with a variety of cellular activities including cellular housekeeping, mitosis, tissue heterogeneity, extracellular matrix synthesis as well as numerous others. Gene clusters "paleturquoise", "darkorange2", and "darkslateblue" are enriched in known extracellular matrix protein markers in AF, while the clusters "black", "grey60", and "lightyellow" are associated with extracellular matrix protein markers characteristic of NP.

Table 1

Extracellular matrix related genes highly expressed in annulus fibrosus

GeneID	Average expression (RPKM) in annulus fibrosus	GeneID	Average expression (RPKM) in annulus fibrosus
COMP	3990.88	SERPINA1	247.96
FN1	3374.09	TIMP2	246.71
CLU	2562.49	CALR	242.68
TPT1	2502.16	CRTAC1	242.53
DCN	2434.52	DPT	204.77
MGP	2270.18	SERPINF1	198.73
LUM	2039.40	SERPING1	186.09
COL1A1	1393.37	CILP2	185.94
SPARC	1386.58	APOE	179.84
FMOD	1325.29	MMP14	175.88
COL1A2	1255.57	TGFBI	174.91
COL2A1	1161.98	POSTN	173.01
CI LP	1126.00	IBSP	168.53
COL3A1	1042.38	IGFBP4	165.21
CST3	972.51	COL9A3	154.93
HTRA1	871.24	SOD3	152.31
BGN	865.06	IGFBP6	145.98
FGFBP2	860.36	SPARCL1	142.91
LGALS1	711.77	SOD1	137.06
SPP1	681.08	BGLAP	135.65
PRELP	640.12	PLA2G2A	134.42
SCRG1	629.02	APOD	131.80
CHAD	614.98	CHI3L2	130.44
COL6A2	567.11	ANGPTL2	127.09
ACAN	564.31	TIMP3	126.93
CTSK	534.82	FSTL1	126.74
TIMP1	469.09	SERPINE2	125.99
GPX3	450.88	ALDOA	125.16
CTGF	433.32	PRDX4	123.56
MMP9	416.09	CCDC80	121.68
IGFBP7	352.81	COL11A2	117.92
PSAP	349.13	COL5A2	112.32
COL6A1	313.96	NUCB1	111.91
ASPN	308.16	A2M	111.41
MFGE8	292.56	COL6A3	106.22
CYTL1	277.74	LGALS3	105.95

GeneID	Average expression (RPKM) in annulus fibrosus	GeneID	Average expression (RPKM) in annulus fibrosus
GSN	277.71	FXYD6	104.61
OGN	259.14	ANXA2	100.74

Table 2

Extracellular matrix related genes highly expressed in nucleus pulposus

GeneID	Average expression (RPKM) in nucleus pulposus	GeneID	Average expression (RPKM) in nucleus pulposus
FN1	6385.17	TIMP2	262.80
COMP	6014.23	CILP2	261.34
CLU	4378.49	CALR	261.25
DCN	3295.38	PLA2G2A	254.91
LUM	3093.90	COL9A3	245.78
MGP	2855.43	TGFBI	242.75
TPT1	2341.70	GSN	242.39
FMOD	2199.02	SERPING1	233.51
COL2A1	1840.27	SERPINE2	226.51
CILP	1626.80	SOD3	201.91
HTRA1	1482.74	IBSP	184.82
FGFBP2	1220.04	CHI3L1	184.64
BGN	1155.23	COL11A2	181.05
SPARC	1065.99	TIMP3	180.53
ACAN	1030.66	CCDC80	175.94
SCRG1	1028.47	COL9A2	168.77
PRELP	989.54	IGFBP6	160.61
COL3A1	940.80	POSTN	158.17
CHAD	835.31	SOD1	155.23
GPX3	643.54	FSTL1	153.32
CTGF	567.45	SPP1	152.31
CHI3L2	541.51	PRDX4	150.92
COL1A2	534.43	FXYD6	147.34
TIMP1	529.60	ANGPTL2	145.53
LGALS1	516.12	IGFBP4	138.17
CRTAC1	475.35	RBP4	137.83
CYTL1	452.88	NUCB1	124.30
CST3	437.51	ALDOA	122.41
COL6A2	430.48	APOE	121.20
SERPINA1	411.25	COL11A1	118.90
OGN	411.25	LGALS3	118.41
PSAP	402.65	APOD	116.58
MFGE8	337.14	COL5A2	116.18
COL1A1	322.44	COL6A3	111.84
ASPN	314.72	CTSK	111.52
DPT	306.39	CRLF1	110.49

GeneID	Average expression (RPKM) in nucleus pulposus	GeneID	Average expression (RPKM) in nucleus pulposus
COL6A1	285.52	ANXA2	103.52
IGFBP7	278.01	MIA	103.03

Table 3

Significant extracellular matrix related genes enriched in annulus fibrosus and nucleus pulposus

Genes enriched in nucleus pulposus		Genes enriched in nucleus pulposus	
CCBE1	collagen and calcium binding EGF domains 1	ACAN	aggrecan
CNTN1	contactin 1	CHI3L1	chitinase 3 like 1
CNTNAP3B	contactin associated protein-like 3B	CHRD	chordin
COL14A1	collagen type XIV alpha 1 chain	COL10A1	collagen type X alpha 1 chain
COL17A1	collagen type XVII alpha 1 chain	COL11A1	collagen type XI alpha 1 chain
COL18A1	collagen type XVIII alpha 1 chain	COL8A2	collagen type VIII alpha 2 chain
COL21A1	collagen type XXI alpha 1 chain	COL9A2	collagen type IX alpha 2 chain
COL24A1	collagen type XXIV alpha 1 chain	CRTAC1	cartilage acidic protein 1
COL4A1	collagen type IV alpha 1 chain	FMOD	fibromodulin
DLL1	delta like canonical Notch ligand 1	FN1	fibronectin 1
DTX1	deltex E3 ubiquitin ligase 1	GPC6	glypican 6
DTX4	deltex E3 ubiquitin ligase 4	HHIPL1	HHIP like 1
EGFLAM	EGF like, fibronectin type III and laminin G domains	HHIPL2	HHIP like 2
JAG1	jagged 1	LAMC3	laminin subunit gamma 3
JAG2	jagged 2	LTBP2	latent transforming growth factor beta binding protein 2
LAMA3	laminin subunit alpha 3	LUM	lumican
LAMA4	laminin subunit alpha 4	OGN	osteoglycin
LAMA5	laminin subunit alpha 5	PRG4	proteoglycan 4
NOTCH3	notch 3	SDC4	syndecan 4
NOTCH4	notch 4	SRPX2	sushi repeat containing protein, X-linked 2
PDGFB	platelet derived growth factor subunit B	WISP3	WNT1 inducible signaling pathway protein 3

Table 4

Annulus fibrosus co-regulatory gene networks

ECM and cell adhesion related genes				Signaling Associated Genes			
Gene symbol	**Gene name**	**Function**	**Cluster**	**Gene symbol**	**Gene name**	**Function**	**Cluster**
ADAM12	ADAM metallopeptidase domain 12	ECM	"paleturquoise"	FGF9	fibroblast growth factor 9	Growth factor	"paleturquoise"
COL5A1	collagen, type V, alpha 1	ECM	"paleturquoise"	KREMEN1	kringle containing transmembrane protein 1	Wnt signaling	"paleturquoise"
COL5A2	collagen, type V, alpha 2	ECM	"paleturquoise"	PDGFRA	platelet-derived growth factor receptor, alpha polypeptide	Growth factor	"paleturquoise"
COL6A3	collagen, type VI, alpha 3	ECM	"paleturquoise"	WISP1	WNT1 inducible signaling pathway protein 1	Wnt signaling	"paleturquoise"
CDH5	cadherin 5, type 2	Adhesion	"darkorange2"	WNT5A	wingless-type MMTV integration site family, member 5A	Wnt signaling	"paleturquoise"
CDH6	cadherin 6, type 2, K-cadherin	Adhesion	"darkorange2"	WNT6	wingless-type MMTV integration site family, member 6	Wnt signaling	"paleturquoise"
CDH24	cadherin-like 24	Adhesion	"darkorange2"	WNT9B	wingless-type MMTV integration site family, member 9B	Wnt signaling	"paleturquoise"
COL17A1	collagen type XVII alpha 1 chain	ECM	"darkorange2"	CDH6	cadherin 6	NOTCH signaling	"darkorange2"
COL18A1	collagen, type XVIII, alpha 1	ECM	"darkorange2"	CDKN1B	cyclin dependent kinase inhibitor 1B	NOTCH signaling	"darkorange2"
COL21A1	collagen, type XXI, alpha 1	ECM	"darkorange2"	DNER	delta/notch like EGF repeat containing	NOTCH signaling	"darkorange2"
COL4A1	collagen type IV alpha 1 chain	ECM	"darkorange2"	HES5	hes family bHLH transcription factor 5	NOTCH signaling	"darkorange2"
COL4A2	collagen type IV alpha 2 chain	ECM	"darkorange2"	HEYL	hes related family bHLH transcription factor with YRPW motif-like	NOTCH signaling	"darkorange2"
COL4A5	collagen type IV alpha 5 chain	ECM	"darkorange2"	HHEX	hematopoietically expressed homeobox	NOTCH signaling	"darkorange2"
CNTN4	contactin 4	Adhesion	"darkorange2"	HOXD3	homeobox D3	NOTCH signaling	"darkorange2"
ELN	elastin	ECM	"darkorange2"	IGFBP4	insulin-like growth factor binding protein 4	Wnt signaling	"darkorange2"
FBLN1	fibulin 1	ECM	"darkorange2"	IGFBP6	insulin-like growth factor binding protein 6	Wnt signaling	"darkorange2"
FBLN5	fibulin 5	ECM	"darkorange2"	IGFBP7	insulin-like growth factor binding protein 7	Wnt signaling	"darkorange2"
ICAM1	intercellular adhesion molecule 1	Adhesion	"darkorange2"	JAG1	jagged 1	NOTCH signaling	"darkorange2"
ICAM2	intercellular adhesion molecule 2	Adhesion	"darkorange2"	JAG2	jagged 2	NOTCH signaling	"darkorange2"
ITGA3	integrin subunit alpha 3	Adhesion	"darkorange2"	KCNA5	potassium voltage-gated channel subfamily A member 5	NOTCH signaling	"darkorange2"
ITGA6	integrin subunit alpha 6	Adhesion	"darkorange2"	MAML3	mastermind like transcriptional coactivator 3	NOTCH signaling	"darkorange2"
ITGA7	integrin subunit alpha 7	Adhesion	"darkorange2"	NEURL1B	neuralized E3 ubiquitin protein ligase 1B	NOTCH signaling	"darkorange2"

ECM and cell adhesion related genes				Signaling Associated Genes			
Gene symbol	**Gene name**	**Function**	**Cluster**	**Gene symbol**	**Gene name**	**Function**	**Cluster**
ITGA8	integrin subunit alpha 8	Adhesion	"darkorange2"	NOTCH3	notch 3	NOTCH signaling	"darkorange2"
ITGA9	integrin subunit alpha 9	Adhesion	"darkorange2"	NOTCH4	notch 4	NOTCH signaling	"darkorange2"
ITGB4	integrin subunit beta 4	Adhesion	"darkorange2"	NRARP	NOTCH-regulated ankyrin repeat protein	NOTCH signaling	"darkorange2"
JAM2	junctional adhesion molecule 2	Adhesion	"darkorange2"	PDGFB	platelet-derived growth factor beta polypeptide	Growth factor	"darkorange2"
LAMA3	laminin subunit alpha 3	Adhesion	"darkorange2"	PTP4A3	protein tyrosine phosphatase type IVA, member 3	NOTCH signaling	"darkorange2"
LAMA4	laminin subunit alpha 4	Adhesion	"darkorange2"	VEGFC	vascular endothelial growth factor C	Growth factor	"darkorange2"
LAMA5	laminin subunit alpha 5	Adhesion	"darkorange2"	WISP2	WNT1 inducible signaling pathway protein 2	Wnt signaling	"darkorange2"
LAMB1	laminin subunit beta 1	Adhesion	"darkorange2"	WISP3	WNT1 inducible signaling pathway protein 3	Wnt signaling	"darkorange2"
LAMB1	laminin subunit beta 1	Adhesion	"darkorange2"	ZNF423	zinc finger protein 423	NOTCH signaling	"darkorange2"
MYH9	myosin heavy chain 9	Adhesion	"darkorange2"				
PCDH1	protocadherin 1	Adhesion	"darkorange2"				
PCDH12	protocadherin 12	Adhesion	"darkorange2"				
PCDH17	protocadherin 17	Adhesion	"darkorange2"				
PCDH19	protocadherin 19	Adhesion	"darkorange2"				
TINAGL1	tubulointerstitial nephritis antigen like 1	Adhesion	"darkorange2"				
ADAMTS7	ADAM metallopeptidase with thrombospondin type 1 motif, 7	ECM	"darkslateblue"				
CNTN1	contactin 1	Adhesion	"darkslateblue"				
COL5A3	collagen, type V, alpha 3	ECM	"darkslateblue"				
COL6A1	collagen, type VI, alpha 1	ECM	"darkslateblue"				
LAMA1	laminin, alpha 1	Adhesion	"darkslateblue"				

Table 5

Nucleus pulposus co-regulatory gene network

ECM and cell adhesion related genes				Signaling associated genes			
Gene symbol	**Gene name**	**Function**	**Cluster**	**Gene symbol**	**Gene name**	**Function**	**Cluster**
CDH26	cadherin-like 26	Adhesion	"black"	CTGF	connective tissue growth factor	Growth factor	"black"
CDHR5	mucin-like protocadherin	Adhesion	"black"	FGFR2	fibroblast growth factor receptor 2	Growth factor	"black"
CELSR3	cadherin, EGF LAG seven-pass G-type receptor 3	Adhesion	"black"	FGFR3	fibroblast growth factor receptor 3	Growth factor	"black"
CILP	cartilage intermediate layer protein, nucleotide pyrophosphohydrolase	ECM	"black"	BMP2	bone morphogenetic protein 2	Growth factor	"grey60"
COL27A1	collagen, type XXVII, alpha 1	ECM	"black"	BMP6	bone morphogenetic protein 6	Growth factor	"grey60"
COL2A1	collagen, type II, alpha 1	ECM	"black"	FGF1	fibroblast growth factor 1 (acidic)	Growth factor	"grey60"
CRTAP	cartilage associated protein	ECM	"black"	FGF2	fibroblast growth factor 2 (basic)	Growth factor	"grey60"
CTGF	connective tissue growth factor	ECM	"black"	GDF6	growth differentiation factor 6	Growth factor	"grey60"
DSCAML1	Down syndrome cell adhesion molecule like 1	Adhesion	"black"	HHIP	hedgehog interacting protein	Growth factor	"grey60"
GPC6	glypican 6	ECM	"black"	IGFBP3	insulin-like growth factor binding protein 3	Growth factor	"grey60"
ITGA10	integrin, alpha 10	Adhesion	"black"	INHBA	inhibin, beta A	Growth factor	"grey60"
LMLN	leishmanolysin-like	Adhesion	"black"	NGF	nerve growth factor (beta polypeptide)	Growth factor	"grey60"
PCDH20	protocadherin 20	Adhesion	"black"	NOG	noggin	Growth factor	"grey60"
TESK2	testis-specific kinase 2	Adhesion	"black"	PDGFC	platelet derived growth factor C	Growth factor	"grey60"
ADAMTS6	ADAM metallopeptidase with thrombospondin type 1 motif, 6	ECM	"grey60"	TGFA	transforming growth factor, alpha	Growth factor	"grey60"
CCDC80	coiled-coil domain containing 80	ECM	"grey60"	TGFBR1	transforming growth factor, beta receptor 1	Growth factor	"grey60"
CDH19	cadherin 19, type 2	Adhesion	"grey60"	TSHB	thyroid stimulating hormone, beta	Growth factor	"grey60"
CHI3L1	chitinase 3-like 1	ECM	"grey60"	VEGFA	vascular endothelial growth factor A	Growth factor	"grey60"
FN1	fibronectin 1	ECM	"grey60"	WNT1	wingless-type MMTV integration site family, member 1	Wnt signaling	"grey60"
HAPLN1	hyaluronan and proteoglycan link protein 1	ECM	"grey60"	WNT16	wingless-type MMTV integration site family, member 16	Wnt signaling	"grey60"
IMPG2	interphotoreceptor matrix proteoglycan 2	ECM	"grey60"	WNT9A	wingless-type MMTV integration site family, member 9A	Wnt signaling	"grey60"
ITGB5	integrin, beta 5	Adhesion	"grey60"	GDF5	growth differentiation factor 5	Growth factor	"lightyellow"

ECM and cell adhesion related genes				Signaling associated genes			
Gene symbol	**Gene name**	**Function**	**Cluster**	**Gene symbol**	**Gene name**	**Function**	**Cluster**
LAMB3	laminin, beta 3	Adhesion	"grey60"	HHIPL1	HHIP-like 1	Hedgehog signaling	"lightyellow"
LUM	lumican	ECM	"grey60"	HHIPL2	HHIP-like 2	Hedgehog signaling	"lightyellow"
PRG4	proteoglycan 4	ECM	"grey60"	INHA	inhibin, alpha	Growth factor	"lightyellow"
SERPINE1	serpin peptidase inhibitor, clade E member 1	ECM	"grey60"	NRG4	neuregulin 4	Growth factor	"lightyellow"
SERPINE2	serpin peptidase inhibitor, clade E member 2	ECM	"grey60"	NRTN	neurturin	Growth factor	"lightyellow"
SMOC1	SPARC related modular calcium binding 1	ECM	"grey60"				
TIMP2	TIMP metallopeptidase inhibitor 2	ECM	"grey60"				
TIMP3	TIMP metallopeptidase inhibitor 3	ECM	"grey60"				
VCAN	versican	ECM	"grey60"				
ACAN	aggrecan	ECM	"lightyellow"				
ADAMTSL2	similar to ADAMTS-like 2; ADAMTS-like 2	ECM	"lightyellow"				
BGN	biglycan	ECM	"lightyellow"				
CHAD	chondroadherin	Adhesion	"lightyellow"				
CILP2	cartilage intermediate layer protein 2	ECM	"lightyellow"				
COL11A2	collagen, type XI, alpha 2	ECM	"lightyellow"				
COL9A2	collagen, type IX, alpha 2	ECM	"lightyellow"				
COL9A3	collagen, type IX, alpha 3	ECM	"lightyellow"				
COMP	cartilage oligomeric matrix protein	ECM	"lightyellow"				
EMILIN3	elastin microfibril interfacer 3	ECM	"lightyellow"				
PRELP	proline/arginine-rich end leucine-rich repeat protein	ECM	"lightyellow"				
SERPINA1	serpin peptidase inhibitor, clade A member 1	ECM	"lightyellow"				
SPINT2	serine peptidase inhibitor, Kunitz type, 2	ECM	"lightyellow"				